

# Multipath-assisted Radio Sensing and Occupancy Detection for Smart In-house Parking in ITS

Jonas Ninnemann<sup>1</sup>, Paul Schwarzbach<sup>1</sup> and Oliver Michler<sup>1</sup>

<sup>1</sup>Chair of Transport Systems Information Technology, Institute of Traffic Telematics, Technische Universität Dresden, 01062 Dresden, Germany

## Abstract

Joint, radio-based communication, localization and sensing is a rapidly emerging research field with various application potentials. Greatly benefiting from these capabilities, smart city, mobility, and logistic concepts are key components for maximizing the efficiency of modern transportation systems. In urban environments, both the search for parking space and freight transport are time- and space-consuming and present the bottlenecks for these transportation chains. Providing location information for these heterogeneous requirement profiles (both active and passive localization of objects), can be realized by using retrofittable wireless sensor networks, which are typically only deployed for active localization. An additional passive detection of objects can be achieved by assessing signal reflections and multipath properties of the transmission channel stored within the Channel Impulse Response (CIR). In this work, a proof-of-concept realization and preliminary experimental results of a CIR-based occupancy detection for parking lots are presented. As the time resolution is dependent on available bandwidth, the CIR of Ultra-wideband transceivers are used. For this, the CIR is smoothed and time-variant changes within it are detected by performing a background subtraction. Finally, the reflecting objects are mapped to individual parking lots. The developed method is tested in an in-house parking garage. The work provided is a foundation for passive occupancy detection, whose capabilities can prospectively be enhanced by exploiting additional physical layers, such as 5G or even 6G.

## Keywords

Channel Impulse Response, Intelligent Transport Systems (ITS), Multipath, Occupancy Detection, Passive Localization, Smart Parking, Traffic Telematics, Ultra-wideband (UWB)

## 1. Introduction

Intelligent transportation systems profit from the interconnection and localization of vehicles, objects, and traffic participants. In this context, location-aware communication is an essential integral part for increasing the efficiency, safety and environmental friendliness of transportation and supply chains. With the rapidly increasing urbanization and growing logistical volumes, intelligent and future-oriented mobility solutions, based on the advancing digitization and technological progress, have to be provided. For this task, concepts for smart cities are studied and discussed [1], where mobility demands are a major challenge. Especially for motorized individual traffic in urban environments, the search for parking space is time-consuming, thus hindering the capabilities of efficient traffic flow management.

*IPIN 2021 WiP Proceedings, November 29 – December 2, 2021, Lloret de Mar, Spain*

✉ Jonas.Ninnemann@tu-dresden.de (J. Ninnemann); Paul.Schwarzbach@tu-dresden.de (P. Schwarzbach); Oliver.Michler@tu-dresden.de (O. Michler)

🆔 0000-0001-7988-079X (J. Ninnemann); 0000-0002-1091-782X (P. Schwarzbach); 0000-0002-8599-5304 (O. Michler)



© 2021 Copyright for this paper by its authors. Use permitted under Creative Commons License Attribution 4.0 International (CC BY 4.0).

CEUR Workshop Proceedings (CEUR-WS.org)

In this context, smart parking systems [2] provide sensor-based and networked solutions to detect parking lot occupancy rates and dispense available capacities in order to minimize parking lot searches. While online smart parking systems offer great potential for compensating the aforementioned issues of urban parking [3, 4], sensory perception of the real-time occupancy rate of available parking space is essential for the performance of smart parking systems. For this task, manifold approaches for providing efficient and reliable occupancy detection of parking space exist, including visual sensor networks with camera via image recognition [5, 6], communication-based via vehicular ad hoc networks [7], crowd sensing by taxis and map/location information [8] or camera-based drone surveillance [9]. More conventional systems typically require parking space selective infrastructure, such as magnetic or infrared [10], or more recently radio-based sensors [11].

Additionally, Wireless Sensor Networks (WSN) provide cheap, long-lasting, and efficient technological solutions for various applications [12], based on the interconnection of devices, while also providing active localization capabilities. Recently, radio-based localization and networking systems focusing on indoor parking have been developed [13], in order to provide cheap and retrofittable solutions for vehicular guidance, occupancy rate and digital billing.

Concurrently to increasing demands on parking space distribution, concepts of further using parking space for logistic applications have been formulated [14]. These provide the idea of additionally using in-house parking lots as so-called mini-hubs for logistical applications to further increase the efficiency of spatial resources by occupying parking space with freight trailers or other storage capabilities.

While this approach leads to increasing capacity optimization, it also changes the demands for localization systems as a basis for occupancy state detection. For the detection of vehicles, active transponders (either the connected vehicle itself, a smartphone, or a connected device at the entrance) are typically required. However, freight trailers or other storage objects are not equipped with these. This hybridization of both active and passive objects within the environment requires additional surveillance capabilities.

In this context, the recently emerging field of joint communication and sensing [15, 16] provides technologically advantageous approaches for this task, as it allows the re-use of radio signals for radar-like applications, e.g. bistatic or multistatic radars [17], and environmental sensing [18], both of which is also referred to as device-free passive localization [19].

This paper focuses on the merging of an already established active localization framework for in-house parking based on Ultra-wideband (UWB), which was presented in [13], and the consecutive use of the transmitted signals by analyzing the Channel Impulse Response (CIR) of the transmission channel. The information on multipath propagation stored in the CIR indicate the presence of reflecting objects, in this special case parking vehicles or trailers, which allow conclusions on the occupancy state of the area (cf. Fig. 1). Furthermore, the UWB CIR can also be used for passive localization of reflecting objects [20, 21].

In order to detect the occupancy of parking space, we use an exponentially weighted moving average (EWMA) filter to smooth the CIR and then perform a background subtraction to detect differences between a static and non-occupied CIR and a potentially occupied measurement input. Subsequently, the detected changes within the CIR are mapped to the environment using an elliptical model and a heatmap representation.

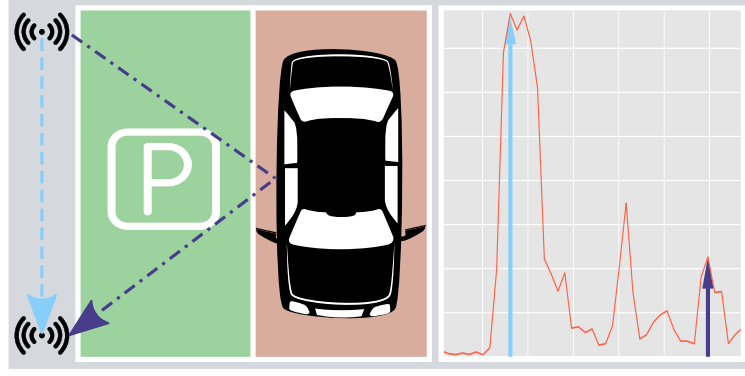


**Figure 1:** Joint communication, localization, and sensing for in-house parking lots: Radio-based passive occupancy detection enabled by mapping the environmentally dependent multipath propagation using the Channel Impulse Response (CIR). The direct and an exemplary reflection path are depicted in light blue and blue in both the site plan (left) and the CIR (right). Free and occupied parking lots are indicated in green and red.

The developed approach is empirically examined in a demanding real-world, in-house parking scenario using a set of UWB transceivers and a minibus, which could potentially represent both parking vehicles and freight trailers. In this context, this paper focuses on the recognizability of the occupation solely derived from the measured CIR and discusses the challenges and limitations of different constellations as well as the examined UWB physical layer.

The rest of the paper is structured as follows: After the introduction in Sec. 1, Sec. 2 presents the passive, radio-based occupancy detection approach as well as necessary inputs and processing steps. Subsequently, Sec. 3 introduce the in-house parking measurement environment and the deployed UWB sensors. The surveyed measurements are presented and discussed in Sec. 4. The paper concludes with a summary and proposals for future work in Sec. 5.

## 2. Multipath-assisted Passive Occupancy Detection

This section presents the proposed passive occupancy detection approach, for which all processing steps are depicted in Fig. 2. These will be briefly discussed in the following.

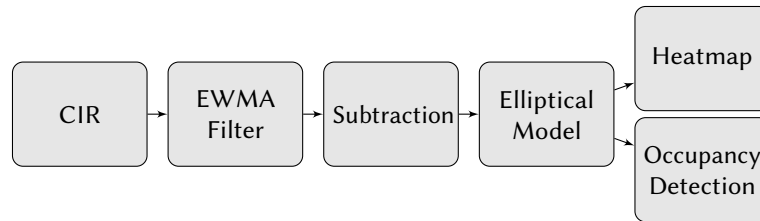


**Figure 2:** Flowchart of multipath-assisted occupancy detection.

## 2.1. Multipath Propagation

The foundation for the proposed passive occupancy detection approach is the multipath propagation phenomenon, where a wireless radio signals reaches the receiver's antenna via multiple paths. In the past, multipath propagation was tried to be mitigated in order to improve the quality of the communication or, for localization tasks, the distance measurements between sensors. However, additional information can be derived by assessing the transfer function of the transmission channel, as reflections are caused by static or dynamic objects within the propagation environment. This leads to the time-delayed reception of additional signal components. Measuring and identifying multipath propagation can be achieved by using large bandwidths. Currently, UWB is a reasonable technological candidate for this task, as pulses with a very short duration are used. The measured multipath components (MPC) are stored within the CIR.

For heavy-multipath environments, such as an in-house parking area, multiple dominant reflection sources are present, e.g. parking vehicles or concrete. A typical multipath propagation in this scenario is given in Fig. 3, which shows the multipath richness of this environment.

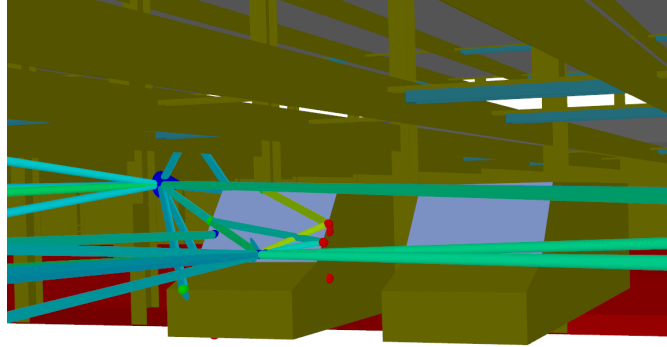


**Figure 3:** 3D Ray-tracing simulation for in-house parking multipath propagation including the transmitting antenna (blue), reflection areas (red dots) and propagation paths (green).

## 2.2. Channel Impulse Response

The CIR represents the time delays caused by the multipath propagation of radio signals. In general, the output  $x(t)$  of a wireless communication system in form of the CIR  $h(t)$  with respect to the input signal  $s(t)$  at time  $t$  can be described as

$$x(t) = h(t) * s(t) + v(t) = \int h(\tau) s(t - \tau) d\tau + v(t), \quad (1)$$

where  $v(t)$  is the additive noise of the signal [22]. Given an impulse input signal, the CIR consists of complex numbers representing the in-phase and quadrature components of the received radio signals. Each value  $k$  is a specific time-shifted impulse  $\delta(t - \tau_k)$ , with  $\delta(\cdot)$  representing the delta function. The CIR is defined in (2), where  $\alpha_k$  and  $\tau_k$  denote the impulse amplitudes and reception time delays [23].

$$h(t) = \sum_{k=1}^K \alpha_k \delta(t - \tau_k) \quad (2)$$

Furthermore, the magnitude of the CIR can be calculated from the obtained complex CIR raw data.

### 2.3. Exponential Weighted Moving Average Filter

In order to reduce the influence of outliers, the CIR is filtered over multiple measurement epochs by applying an EWMA filter. Additionally, EWMA filter can be used to extract static backgrounds in dynamic scenarios [24].

The averaged CIR  $z_t$  at time  $t$  is computed using the previous one  $z_{t-1}$  and the newly received CIR  $h_t$ . The parameter  $\alpha$  in (3) represents a constant scalar weighting factor [25], which for the described use case was set to  $\alpha = 0.3$ . Due to the static environment the  $n = 300$  CIR measurements per scenario are averaged with a small window size of  $k = 5$  by the EWMA filter.

$$z_t = \alpha h_t + (1 - \alpha) z_{t-1} \quad (3)$$

Fig. 4 depicts EMWA results for two different scenarios, including the standard deviation of the filtered results.

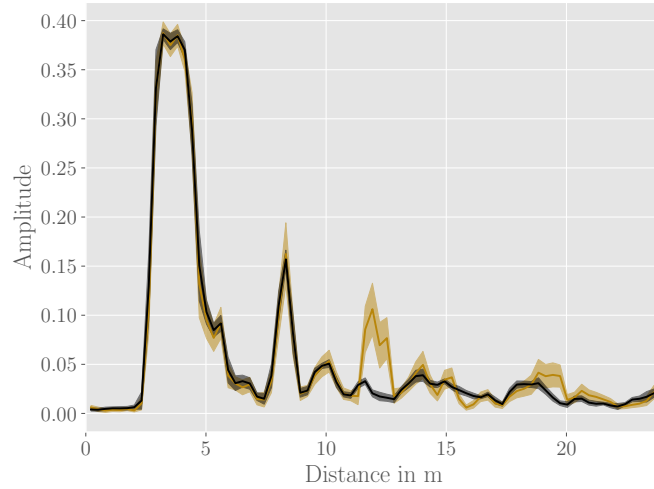


**Figure 4:** EWMA filtered CIR with (golden) and without (black) vehicle ( $n = 300$ ).

### 2.4. Background Subtraction

In complex, real-world scenarios an identification of reflecting sources can be spatially ambiguous if no prior information is available. For this reason, we follow a background subtraction

$s_t$  approach for each measurement epoch  $t$ , which aims at removing static components of the compared CIRs [24, 26]. This can be achieved by comparing the filtered CIR  $z_t^1$  with a previously surveyed reference CIR  $z_t^0$ , which represents a non-occupied scene.

$$s_t = |z_t^1 - z_t^0| \quad (4)$$

In order to provide a correct overlaying of the compared CIRs, they are synchronized via the direct path and the corresponding index. Therefore, they are synced at the leading edge, which is located in the flank of the peak of the direct signal path. In addition, the amplitude values of the filtered CIRs are normalized for a better comparability. Fig. 5 illustrates the subtraction of the CIRs, where both the direct path and an estimation of the reflection path at a target object are also marked. The estimation of the reflection path is obtained as the maximum of  $s_t$ .

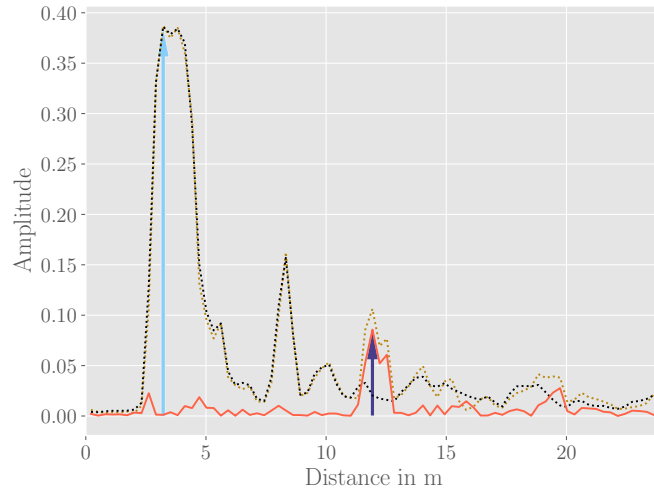


**Figure 5:** Subtracted CIR (red) with  $z_t^1$  (golden) and without vehicle  $z_t^0$  (black), including the direct path (light blue) and the estimated reflection path (blue).

## 2.5. Elliptical Model and Mapping

For the detection of the target vehicle, the time/distance information from the CIR are mapped into a plane. Fig. 6 depicts a graphical overview of the corresponding processing steps. The mapping is realized with an elliptical model, which geometrically represents the positional line of the reflection source, given a bistatic setup and the measured path length from the subtracted CIR  $s_t$ . The position of the transmitter  $\mathbf{X}_T = (x_T, y_T)^\top$  and the receiver  $\mathbf{X}_R = (x_R, y_R)^\top$  within the communication network have to be known in order to detect the target vehicle  $\mathbf{X} = (x, y)^\top$ . Eq. (5) represents the length of the reflection path or the bistatic range  $d_r$ .

$$d_r = \|\mathbf{X}_T - \mathbf{X}\|_2 + \|\mathbf{X}_R - \mathbf{X}\|_2 \quad (5)$$

The bistatic range  $d_r$  is calculated from the CIR via the corresponding time delay  $\tau$  in the CIR for the reflection path and the speed of light  $c$ :

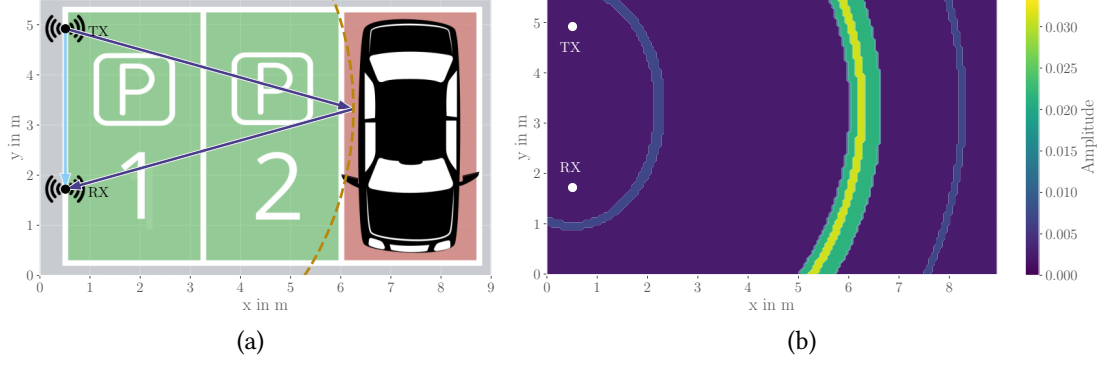


**Figure 6:** CIR mapping: **(a)** Mapping of the reflection path (blue); **(b)** Heatmap of the environment.

$$d_r = \tau \cdot c. \quad (6)$$

Eq. (5) describes an ellipse with the transmitter and the receiver located in the foci. The semi-major axis  $a$  is calculated with the help of the measured bistatic range  $d_r$  and the semi-minor axis  $b$  with the direct path length  $d_p$ .

$$a = \frac{d_r}{2} \quad b = \sqrt{a^2 - \left(\frac{d_p}{2}\right)^2} \quad (7)$$

The two estimated axis of the ellipse allow setting up the parametric equation of the ellipse and therefore the mapping of the reflection path, which is qualitatively shown in Fig. 6a.

As aforementioned, every individual values stored within the CIR represents a potential reflection source, hence all CIR values with their corresponding time delay and amplitude are represented as ellipses with the same foci but different semi-major axis.

In addition, the family of ellipses can be used to provide a representation of the propagation environment and its reflecting sources by performing an environmental mapping. In [20], we proposed the creation of a heatmap based on the time delays and amplitudes of each CIR value. The resulting continuous value surface of the heatmap is obtained by performing a nearest neighbor interpolation and shown in Fig. 6b. Given the example in Fig. 6, a spatial identification of the target vehicle can be achieved. With multiple CIR measurements between different anchors an unambiguous localization of the reflecting object is also possible. [20]

## 2.6. Occupancy Detection

The occupancy detection is performed on the basis of the estimated reflection path from the subtracted CIR. For this purpose, an interval of the reflection path length with respect to the sensor arrangement is calculated for each parking lot. Afterwards the estimated reflection path length and the intervals are compared in order to assign them to a parking lot. For example an estimated reflection path length between 11 m and 17 m indicates a vehicle on parking lot P3. For the empirical evaluation, the occupancy detection state is estimated over all measurement epochs and expressed as the number of correct assignments.

### 3. In-house Parking Measurements

The conducted measurements were carried out in an in-house parking garage, representing a challenging environment for wireless-enabled localization systems. Based on an already established active UWB-based positioning system, the developed approach can further enable occupancy detection and therefore benefit smart parking systems. The testbed for this is an underground parking garage located in Dresden, Germany with over 1000 available parking spaces on two floors [27] (cf. Fig. 7a). Each parking lot is 2.75 m wide and 5.0 m long. The target object for the occupancy detection is a minibus with a size of 5.3 m x 2 m x 2 m.



**Figure 7:** Measurement setup: (a) Parking garage; (b) *Decawave* EVB1000 UWB Transceiver.

The CIR measurements are carried out with *Decawave* EVB1000 Transceivers (cf. Fig. 7b), equipped with a micro-controller and the *Decawave* DW1000 radio chip. For the conducted measurements the parameters in Tab. 1 were applied.

**Table 1**

Measurement Parameters of the DW1000.

Parameter	Value
Center frequency	4492.8 MHz
Bandwidth	499.2 MHz
Pulse repetition frequency (PRF)	16 MHz
Preamble length	1024
Data rate	850 kbps
CIR time resolution $\Delta t \approx$	1 ns or 30 cm

The UWB transceivers were attached to tripods at a height of 1.5 m and connected to a laptop. For this preliminary measurement campaign, two transceivers are deployed to record the CIR raw data, which consists of 992 complex, evenly separated values. With regard to the available bandwidth, the time resolution amounts to  $\Delta t \approx 1$  ns or 30 cm.



## 4. Results

For the empirical validation of the proposed method in a demanding real-world scenario, an in-house parking environment and a minibus was chosen, in order to provide a proof-of-concept for passive vehicle or freight trailer detection based on the CIR. Therefore, the focus of the investigated scenarios is on three parking lots and the correct assignment of the occupancy detection state. In addition, the effect of the EWMA filter is validated. The parking lots are numbered with P1, P2, and P3 to distinguish them in the scenarios.

In the first configuration, the transceivers are placed on the side of the vehicle, as shown in Fig. 8c. The transmitter and the receiver are 3.2 m apart and located at the edge of P1. Three different measurement runs were carried out with this arrangement:

1. Empty parking lots for CIR calibration ( $z_t^0$ ),
2. with a minibus on P2 (cf. Fig. 8) and
3. with a minibus on P3 (cf. Fig. 6).

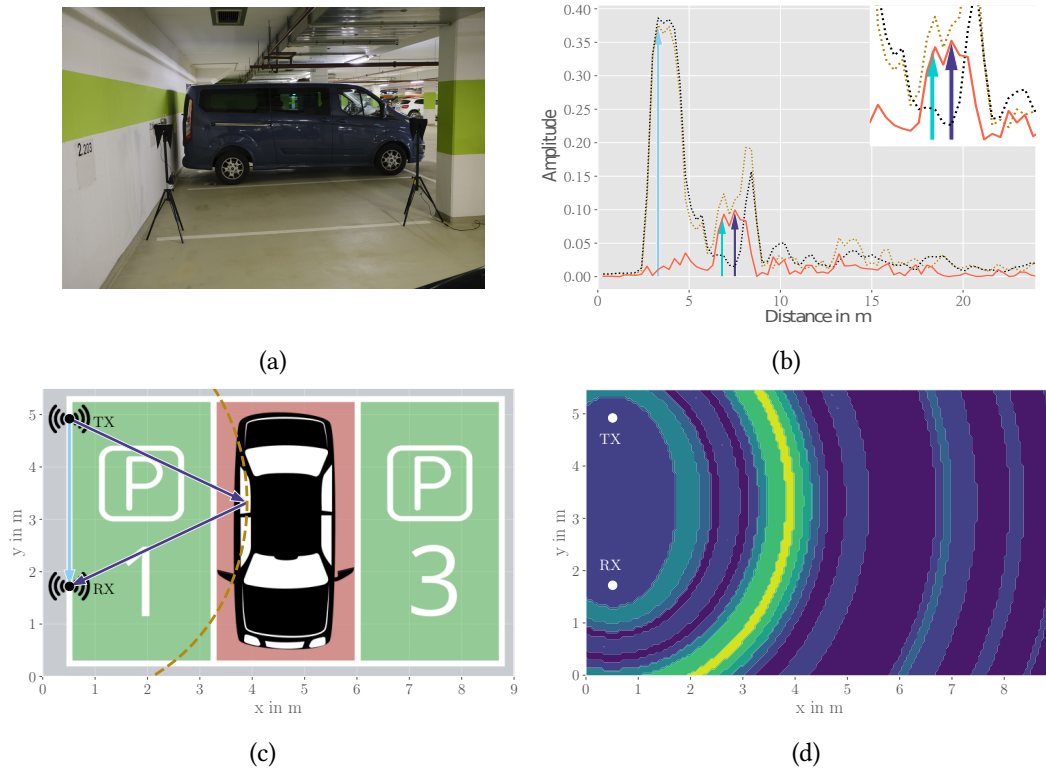


**Figure 8:** Occupancy detection for parking lot P2: (a) CIRs with subtraction with reference reflection path (cyan); (b) Environment with the minibus; (c) Site plan with estimated reflection path (blue); (d) Interpolated Heatmap.

#### 4.1. Minibus on P2

The results of the detection steps for this scenario are shown in Fig. 8. Based on the geometric arrangement the reference reflection path length at the vehicle is 6.8 m.

For the estimation of the reflection path length from the CIR, the EMWA filter and the background subtraction are applied. Here the subtraction is capable of removing other reflections from the environment in order to focus only on the variant reflections when compared to  $z_t^0$ . The estimated reflection path is 7.5 m long, which allows a clear mapping and detection of the vehicle. The deviation to the reference reflection length is potentially caused by multiple reflections at the vehicle, as the subtracted CIR in Fig. 8b indicates. Also, the CIR uncovers a second reflection with only a slightly larger path length for both measurements. With help of the subtraction it is possible to remove this MPC from the CIR.

The mapping of the estimated reflection path with the elliptical model is shown in Fig. 8c alongside with the interpolated heatmap based on all values from the subtracted CIR in Fig. 8d. It visualizes the detection approach with the help of an interval of the estimated reflection path length for every parking lot. In this case the detection indicated an occupancy of the parking lot P2. The empirical evaluation of the detection ratio over all measurement epochs is visualized in Fig. 9a. For the discussed scenario P2, the detection ratio is 97 % when applying the EWMA filter, compared to only 77 % solely based on the unfiltered CIR. This shows the smoothing and outlier removing effects of the EMWA (cf. Fig. 9b), allowing a more robust occupancy detection.

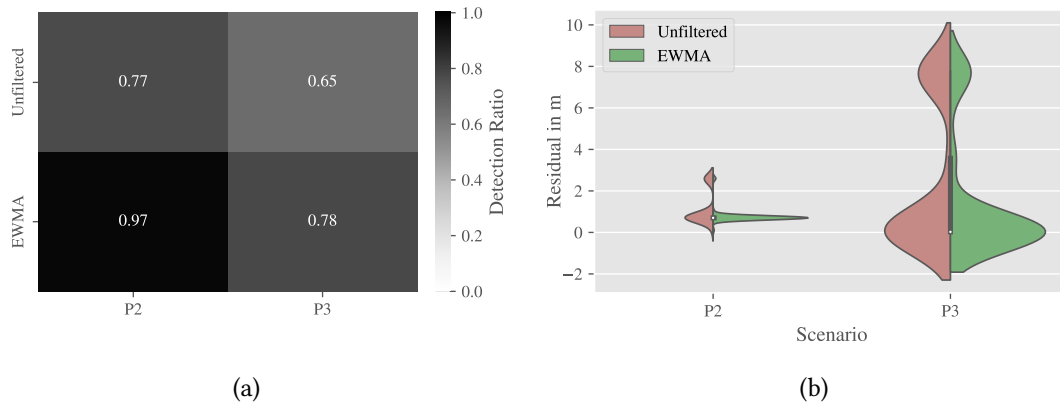


**Figure 9:** Detection: **(a)** Detection Ratio Matrix; **(b)** Violin Plot: Unfiltered reflection path detection (red) and detection after EWMA filter of the CIR (green).

#### 4.2. Minibus on P3

The previously discussed scenario in Fig. 6 (cf. Sec. 2) depicts the detection scenario with the minibus on parking lot P3. For this scenario the reference reflection path length is 11.84 m. From the corresponding CIRs in Fig. 5 a reflection path length of 11.93 m can be estimated.

The background subtraction here eliminates a strong reflection, potentially originating from another vehicle in the environment and therefore allows the focus on the target object on P3. Another effect can be observed from Fig. 4, where at 19 m a double reflection becomes visible.

The signal reflected at the target object is not only received via a single reflection, but also via a second reflection. In this case the subtraction also estimates the double reflection for the vehicle detection. In order to address this problem the number of used sensors should be increased to improve the robustness of the detection.

The mapping and heatmap (Fig. 6) of the subtracted CIR show a clear reflection at the minibus on P3. However, the detection rate (Fig. 9a) with 78 % is lower when compared to the P2 scenario. This is also supported by Fig. 9b, which depicts the residuals between the reference reflection lengths and the estimated lengths for both scenarios. For this, the aforementioned ambiguity for the reflection path in this scenario is revealed.

### 4.3. Resolution and Shadowing

In order to further validate the occupancy detection, an additional transceiver arrangement is further examined. In these scenarios, the UWB modules are placed to cover the same three parking lots, but now along the wall, separated by 8.25 m (cf. Fig. 10a). Again, the calibration measurements were carried out without a vehicle and afterwards the minibus was parked on P2. This arrangement with the transceivers mounted at the walls is also more in line with a WSN for active localization. Additionally, it theoretically provides the capability to cover multiple parking lots and hence higher the coverage of the occupancy detection approach.

Furthermore, the CIR in Fig. 10c indicates some limitations of the conducted measurement setup. Firstly, the separation of the direct and the reflection path in the CIR is examined. In this scenario the reference reflection path length is 8.4 m, which is only 0.15 m longer than the direct path. This path difference is not resolvable in the CIR with a resolution of 0.3 m. The presences of the vehicle only results in a slightly wider direct path peak in the CIR, which is visible after the subtraction. From this it can be deduced that a minimum difference in the path lengths is required in order to separate them in the CIR. This is due to the bandwidth restrictions of the applied technology. For future transmission systems with higher available bandwidth, this shortcoming can potentially be compensated.

Another arising issue might be additional reflections, which can only be measured without the vehicle, but are blocked in the presence of it. This can be observed in Fig. 10c (blue), where a reflection path lengths of 13 m is estimated. A similar effect occurs in the field of camera-based object detection approaches, where shadowing within the images disturb the detection [28].

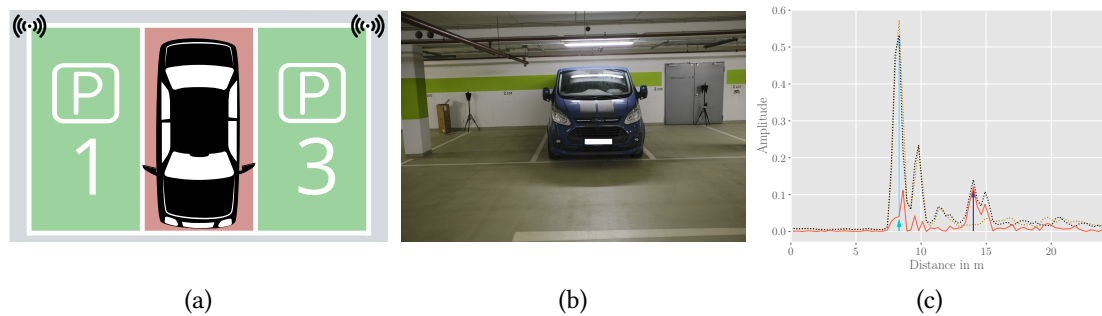


**Figure 10:** Scenario with transceivers along the wall: **(a)** Site plan; **(b)** Environment with vehicle; **(c)** CIRs with subtraction.

## 5. Conclusion & Future Work

The rapidly increasing urbanization and associated demands on mobility and logistics are a challenging task for the upcoming years. With the help of digitization and networking, innovative, low-cost, and retrofittable systems can be established to tackle these tasks. Joint communication, localization, and sensing based on wireless transmission systems provide a promising, efficient, and innovative solution approach for these application fields, e.g. smart cities and parking. Therefore, this contribution presented a remote sensing approach based on multipath information to provide a passive occupancy detection for spatial resources like parking areas or mini-hubs.

The proposed method uses CIR multipath data provided by the transmission modules in order to identify reflections within the propagation environment. To do so, we applied an EMWA filtering and background subtraction method to smooth the CIR and remove invariant components of it. The resulting CIR is then mapped to the environment using an elliptical model and an interpolated heatmap. Based on the reflection estimation, an occupancy detection for individual parking lots is derived.

Comparable occupancy detection technologies and methods (infrared, ultrasonic, camera) are dedicated for a single parking lot. With our setup we were able to observe recognizability of reflection with approximate 25 m path length. For the coverage of an entire parking garage a comparably high number of devices would be required. However, the installed cooperative sensors serve a multi use purposes (joint communication, active localization, passive sensing) and therefore are more cost-efficient when compared to state-of-the-art occupancy detection systems.

For an application-close validation, preliminary field tests with a simplified measurement setup were conducted. The results revealed a proof-of-concept recognition of parking objects for limited constellations and therefore allowed a reliable occupancy detection rate. However, we also discussed the shortcomings of the used UWB technology as well as shadowing effects.

Further research will focus on an extended measurement campaign, including a network of UWB transceivers, allowing ambiguities to be resolved and providing redundant measurements to increase the robustness of the method. Also, detection of multiple objects in a wider range of scenarios will also be considered. Additionally, the use of beam-steering antenna for a better distinction between reflections is proposed.

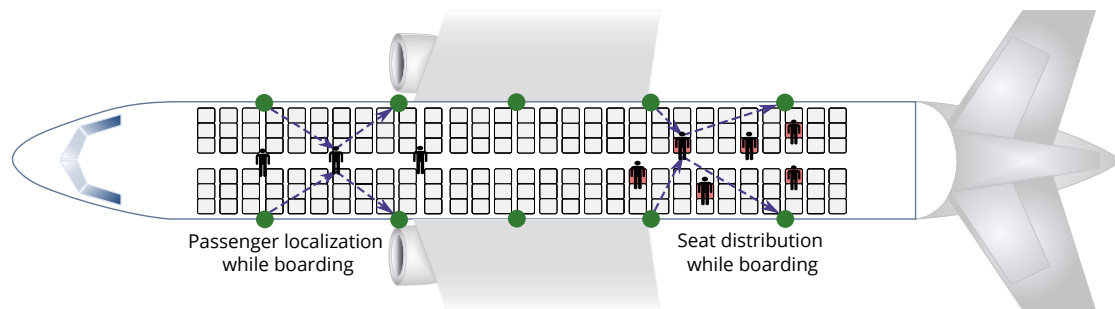


**Figure 11:** Future localization and detection radar system (green) in the connected aircraft cabin (Airbus A320) with passenger localization and seat distribution while boarding.

In the future, a transfer of the approach to other physical layers, with advantageous properties, such as 5G/6G or Li-Fi, will be examined. In addition, validation could be extended to other environments and applications in ITS like the connected aircraft cabin [29], where passive occupancy detection can be beneficial. Figure 11 proposes a future cabin localization system based on the same multipath-assisted detection of people while boarding. This solution monitors the entire boarding process using a single WSN with communication [30], active localization [31] and radio sensing/passive detection.

## 6. Acknowledgments

This work has been supported by the European Union and the State of Saxony within the project "IVS-AMP" as well as by the Federal Ministry for Economic Affairs and Energy of Germany within the project "CABINET".



## References

- [1] A. Kiritat, O. Krejcar, A. Kertesz, M. F. Tasgetiren, Future trends and current state of smart city concepts: A survey, *IEEE Access* 8 (2020) 86448–86467.
- [2] T. Lin, H. Rivano, F. Le Mouél, A survey of smart parking solutions, *IEEE Transactions on Intelligent Transportation Systems* 18 (2017) 3229–3253.
- [3] S. Di Martino, V. N. Vitale, F. Bock, Comparing different on-street parking information for parking guidance and information systems, in: 2019 IEEE Intelligent Vehicles Symposium (IV), 2019, pp. 1093–1098.
- [4] M. K. M. Rabby, M. M. Islam, S. M. Imon, A review of iot application in a smart traffic management system, in: 2019 5th International Conference on Advances in Electrical Engineering (ICAEE), 2019, pp. 280–285.
- [5] L. Baroffio, L. Bondi, M. Cesana, A. E. Redondi, M. Tagliasacchi, A visual sensor network for parking lot occupancy detection in smart cities, in: 2015 IEEE 2nd World Forum on Internet of Things (WF-IoT), 2015, pp. 745–750.
- [6] G. T. S. Ho, Y. P. Tsang, C. H. Wu, W. H. Wong, K. L. Choy, A computer vision-based roadside occupation surveillance system for intelligent transport in smart cities, *Sensors* 19 (2019) 1796.
- [7] M. Caliskan, A. Barthels, B. Scheuermann, M. Mauve, Predicting parking lot occupancy in vehicular ad hoc networks, in: 2007 IEEE 65th Vehicular Technology Conference - VTC2007-Spring, 2007, pp. 277–281.

- [8] F. Bock, S. Di Martino, A. Origlia, Smart parking: Using a crowd of taxis to sense on-street parking space availability, *IEEE Transactions on Intelligent Transportation Systems* 21 (2020) 496–508.
- [9] S. Sarkar, M. W. Totaro, K. Elgazzar, Intelligent drone-based surveillance: application to parking lot monitoring and detection, in: C. M. Shoemaker, H. G. Nguyen, P. L. Muench (Eds.), *Unmanned Systems Technology XXI*, volume 11021, International Society for Optics and Photonics, SPIE, 2019, pp. 13 – 19. URL: <https://doi.org/10.1117/12.2518320>.
- [10] V. Paidi, H. Fleyeh, J. Håkansson, R. Nyberg, Smart parking sensors, technologies and applications for open parking lots: A review, *IET Intelligent Transport Systems* 12 (2018).
- [11] P. Solic, R. Colella, L. Catarinucci, T. Perkovic, L. Patrono, Proof of presence: Novel vehicle detection system, *IEEE Wireless Communications* 26 (2019) 44–49.
- [12] F. Zafari, A. Gkelias, K. K. Leung, A survey of indoor localization systems and technologies, *IEEE Communications Surveys Tutorials* 21 (2019) 2568–2599.
- [13] A. Jung., P. Schwarzbach., O. Michler., Future parking applications: Wireless sensor network positioning for highly automated in-house parking, in: *Proceedings of the 17th International Conference on Informatics in Control, Automation and Robotics - ICINCO*, 2020, pp. 710–717.
- [14] L. Faugère, C. White, B. Montreuil, Mobile access hub deployment for urban parcel logistics, *Sustainability* 12 (2020).
- [15] J. A. Zhang, M. L. Rahman, K. Wu, X. Huang, Y. J. Guo, S. Chen, J. Yuan, Enabling joint communication and radar sensing in mobile networks – a survey, 2021. [arXiv:2006.07559](https://arxiv.org/abs/2006.07559).
- [16] A. Bourdoux, A. N. Barreto, B. van Liempd, C. Lima, D. Dardari, D. Belot, E.-S. Lohan, G. Seco-Granados, H. Sarieddeen, H. Wymeersch, J. Suutala, J. Saloranta, M. Guillaud, M. Isomursu, M. Valkama, M. Aziz, R. Berkvens, T. Sanguanpuak, T. Svensson, Y. Miao, 6g white paper on localization and sensing (2020).
- [17] O. Kanhere, S. Goyal, M. Beluri, T. S. Rappaport, Target localization using bistatic and multistatic radar with 5g nr waveform, 2021. [arXiv:2103.03426](https://arxiv.org/abs/2103.03426).
- [18] C. B. Barneto, E. Rastorgueva-Foi, M. F. Keskin, T. Riihonen, M. Turunen, J. Talvitie, H. Wymeersch, M. Valkama, Radio-based sensing and environment mapping in millimeter-wave 5g and beyond networks, 2021. [arXiv:2102.11593](https://arxiv.org/abs/2102.11593).
- [19] S. Jovanoska, R. Zetik, R. Thomä, F. Govaers, K. Wild, W. Koch, Device-free indoor localization using a distributed network of autonomous UWB sensor nodes, *2013 Workshop on Sensor Data Fusion: Trends, Solutions, Applications, SDF 2013* (2013).
- [20] J. Ninnemann, P. Schwarzbach, A. Jung, O. Michler, Lab-based evaluation of device-free passive localization using multipath channel information, *Sensors* 21 (2021).
- [21] M. Cimdins, S. O. Schmidt, H. Hellbrück, MAMPI-UWB—multipath-assisted device-free localization with magnitude and phase information with UWB transceivers, *Sensors* 20 (2020) 7090.
- [22] X. Jiang, W.-J. Zeng, E. Cheng, C.-R. Lin, Multipath Channel Estimation Using Fast Least-Squares Algorithm, *Proceedings - 2011 3rd International Conference on Communications and Mobile Computing, CMC 2011* (2011) 436.
- [23] B. Matthews, S. O. Schmidt, H. Hellbrück, Understanding and Prediction of Ultra-Wide Band Channel Impulse Response Measurements, *Proceedings of the 4th KuVS/GI Expert Talk on Localization* (2019).

- [24] S. Jovanoska, F. Govaers, R. Thomä, People tracking and data fusion for UWB radar applications, in: R. Klemm, U. Nickel, C. Gierull, P. Lombardo, H. Griffiths, W. Koch (Eds.), *Novel Radar Techniques and Applications Volume 2: Waveform Diversity and Cognitive Radar, and Target Tracking and Data Fusion*, Institution of Engineering and Technology, 2017, pp. 429–455.
- [25] S. Jovanoska, R. Thoma, Multiple target tracking by a distributed uwb sensor network based on the phd filter, in: *2012 15th International Conference on Information Fusion*, 2012, pp. 1095 – 1102.
- [26] S. H. Shaikh, K. Saeed, N. Chaki, Moving object detection using background subtraction, in: *Moving Object Detection Using Background Subtraction*, Springer International Publishing, Cham, 2014, pp. 15–23.
- [27] W. T. C. Dresden, Parking at the wtc dresden, 2021. URL: <https://wtc-dresden.de/en/parking.html>.
- [28] R. Barbuzza, L. Dominguez, A. Perez, L. F. Esteberena, A. Rubiales, J. P. D’amato, A shadow removal approach for a background subtraction algorithm, in: A. E. De Giusti (Ed.), *Computer Science – CACIC 2017*, Springer International Publishing, Cham, 2018, pp. 101–110.
- [29] P. Schwarzbach, J. Engelbrecht, A. Michler, M. Schultz, O. Michler, Evaluation of technology-supported distance measuring to ensure safe aircraft boarding during covid-19 pandemic, *Sustainability* 12 (2020). URL: <https://www.mdpi.com/2071-1050/12/20/8724>. doi:10.3390/su12208724.
- [30] J. Engelbrecht, T. Fuss, U. Schwark, O. Michler, Measurement of interference path loss between wireless avionics intra-communications system and aircraft systems at 4.2-4.4 ghz band, in: *2014 Loughborough Antennas and Propagation Conference (LAPC)*, 2014, pp. 119–123. doi:10.1109/LAPC.2014.6996335.
- [31] J. Ringel, S. Klippahn, O. Michler, Simulation of wave propagation for radio and positioning planning inside aircraft cabins, in: *Proceedings of the 3rd International Conference on Models and Technologies for Intelligent Transportation Systems (MT-ITS 2013)*, Dresden, 2013, pp. 243–253.